AD-A093 166 CONNECTICUT UNIV STORRS INST OF MATERIALS SCIENCE F/G 11/4
WEAR OF HOMOGENEOUS AND COMPOSITE MATERIALS UNDER CONDITIONS OF--ETC(U)
1980 S RICE, R SOLECKI, H NOWOTNY F49620-79-C-0221
UNCLASSIFIED AFOSR-TR-80-1195 NL

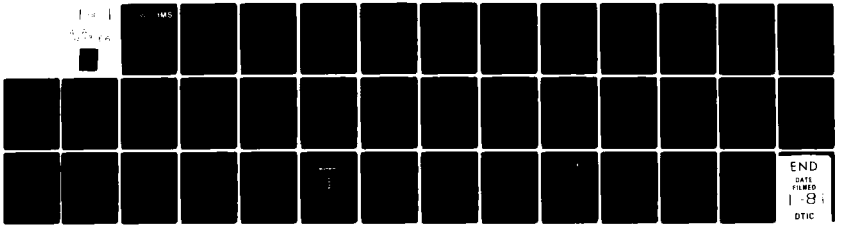

END
DATE FILMED
1-81
DTIC

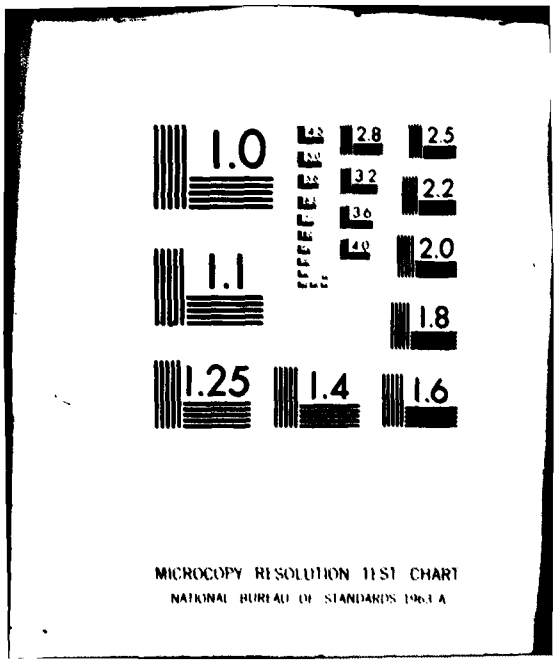
1.0
1.1
1.25
1.4
1.6
1.8
2.0
2.2
2.5
2.8
3.2
3.6
4.0
MICROCOPY RESOLUTION TEST CHART
NATIONAL BUREAU OF STANDARDS 1963 A

LEVEL II

(9)

IMS

INSTITUTE OF MATERIALS SCIENCE

Final Scientific Report

to

United States Air Force
Air Force Office of Scientific Research

Wear of Homogeneous and Composite Materials
Under Conditions of Repeated Normal and
Sliding Impact

AFOSR-TR-80-

F49620-79-C-0221

Approved for public release; distribution unlimited.

THE UNIVERSITY OF CONNECTICUT
Storrs · Connecticut

Final Scientific Report

to

United States Air Force
Air Force Office of Scientific Research

Wear of Homogeneous and Composite Materials
Under Conditions of Repeated Normal and
Sliding Impact

AFOSR-TR-80-

UNCLASSIFIED

REPORT DOCUMENTATION PAGE

READ INSTRUCTIONS BEFORE COMPLETING FORM

1. REPORT NUMBER 19 (12) AFOSR-TR-80-1195	2. GOVT ACCESSION NO. AD-A093 766
3. RECIPIENT'S CATALOG NUMBER	
4. TITLE (and Subtitle) Wear of Homogeneous and Composite Materials under Conditions of Repeated Normal and Sliding Impact,	5. TYPE OF REPORT & PERIOD COVERED FINAL
	6. PERFORMING ORG. REPORT NUMBER
7. AUTHOR(s) (10) Stephen Rice, Roman Solecki, Hans Nowotny	8. CONTRACT OR GRANT NUMBER(s) (15) F49620-79-C-0221
9. PERFORMING ORGANIZATION NAME AND ADDRESS University of Connecticut, Mechanical Engineering Department, Storrs, Connecticut 06268 (12) 39	10. PROGRAM ELEMENT, PROJECT, TASK AREA & WORK UNIT NUMBERS (11) 2307/B2 (17) 61102F
11. CONTROLLING OFFICE NAME AND ADDRESS Air Force Office of Scientific Research/NA, Bldg. 410, Bolling Air Force Base, D.C. 20332 (11)	12. REPORT DATE 1980
	13. NUMBER OF PAGES 34
14. MONITORING AGENCY NAME & ADDRESS (if different from Controlling Office) (9) Final Rept.	15. SECURITY CLASS. (of this report) UNCLASSIFIED
	15a. DECLASSIFICATION/DOWNGRADING SCHEDULE

16. DISTRIBUTION STATEMENT (of this Report)

Approved for public release; distribution unlimited.

17. DISTRIBUTION STATEMENT (of the abstract entered in Block 20, if different from Report)

18. SUPPLEMENTARY NOTES

19. KEY WORDS (Continue on reverse side if necessary and identify by block number)

WEAR	SUBSURFACE ZONES	STRESS	FRICTION
SLIDING	WEAR TESTING METHODOLOGY	ENVIRONMENT	
IMPACT	WEAR MECHANISMS	TEMPERATURE	
EXPERIMENTAL	DETERMINISTIC VARIABLES	STIFFNESS	
ANALYTICAL	VELOCITY	SOLID CONTACT	

20. ABSTRACT (Continue on reverse side if necessary and identify by block number)

This report describes experimental and analytical investigations in the area of wear of materials under repetitive impulsive and sliding contact. Both pin-on-disc and impact wear test machines have been utilized in conducting experiments involving solid contact between specimen and counterface materials.

The report includes a description of experimental methodology employed in research in wear, and enumerates the considerations relevant to a given experiment. Further noted are the deterministic external variables which

DD FORM 1473 1/0679/6 UNCLASSIFIED

serve to define operative wear regimes and processes. These variables include velocity, stress, test duration, environment and the effective mechanical stiffness of the specimen/counterface contact.

Specific experimental results which illustrate phenomenologically distinct wear behaviors which arise due to differing levels in external variables are highlighted. The importance of these findings to further research in impact and sliding wear is noted.

Analytical work has focused on the determination of states of stress and strain in material specimens undergoing repetitive impact. In particular, a bar striking an elastic half-space and a cylinder contacting a moving, rough, rigid plane were studied in some detail. These analytical results are applicable to the study of in situ material "processing" during wear, and to the formation of subsurface zones arising both in impact and sliding wear.

Abstract

This report describes experimental and analytical investigations in the area of wear of materials under repetitive impulsive and sliding contact. Both pin-on-disc and impact wear test machines have been utilized in conducting experiments involving solid contact between specimen and counterface materials.

The report includes a description of experimental methodology employed in research in wear, and enumerates the considerations relevant to a given experiment. Further noted are the deterministic external variables which serve to define operative wear regimes and processes. These variables include velocity, stress, test duration, environment and the effective mechanical stiffness of the specimen/counterface contact.

Specific experimental results which illustrate phenomenologically distinct wear behaviors which arise due to differing levels in external variables are highlighted. The importance of these findings to further research in impact and sliding wear is noted.

Analytical work has focused on the determination of states of stress and strain in material specimens undergoing repetitive impact. In particular, a bar striking an elastic half-space and a cylinder contacting a moving, rough, rigid plane were studied in some detail. These analytical results are applicable to the study of in situ material "processing" during wear, and to the formation of subsurface zones arising both in impact and sliding wear.

(AFSC)

nd is
(7b).

Introduction

This report follows those written earlier on investigations in the area of wear of materials under impulsive loading [1-3]. During the course of this project, a considerable amount of experimental and analytical work has been accomplished. For the most part, results from these investigations have been (or are being) published, and the interested reader is referred to the literature for detailed information [4-20,28,29].

Accordingly, the purpose of this report is to present (a) an overview on simulative impact wear experimentation and methodology, and (b) highlight pertinent findings and developments obtained during the period 1 September 79 - 31 August 80.

Experimental

Figure 1 presents a diagram which illustrates some of the factors important in conducting simulative wear tests and in analyzing results obtained in such experimentation. The complexity of the figure suggests that there is considerably more involved in performing a "wear test" than in simply rubbing two surfaces together and measuring "weight loss". Indeed, this is the purpose for presenting this figure, and it is useful to review a few aspects explicitly.

The first question confronting the experimentalist is to select materials for the test. In some cases, a particular material or material pair (specimen plus counterface) is suggested due to "external considerations." For example, a manufacturer of stainless steels needs to establish some empirical relative information concerning the wear resistance of a series of such steels against given counterface materials under given conditions of solid or lubricated contact. In basic research, however, the question of which materials to test

should devolve to a rational scientific hypothesis. In cases where a variety of materials is to be tested, the selection of particular materials might be on the basis of microstructures attractive for the extent to which metallographic detail can be resolved with given instrumentation. In any case, the significant point is that selection of material pairs for test is an important factor which should be given due consideration a priori. Further, the rational basis for material selection should be noted when experimental results are published.

Following selection of materials, Figure 1 notes that specimen preparation occurs. It is noteworthy that this preparation involves a series of steps, depending upon the particular nature of specimen and counterface materials. With most materials, specimens must be machined to a configuration adaptable to the wear test apparatus. Following this, specimens are often polished or finish-machined by some other means. In any case, it is important to obtain "baseline" specimens following this initial preparation. Such baseline samples should be examined for surface and subsurface features to document the initial condition of both specimen and counterface materials. This avoids the introduction of artifacts prior to test, which otherwise might be construed as having arisen during the wear test itself.

The third major consideration prior to wear testing is the selection of "external parameters". The identification and specification of these variables has been an important part of the research documented in various articles resulting from our recent work in impact wear [6-10]. While alternative descriptions are possible, the external parameters of consequence have been shown to be nominal contact stress, transverse relative sliding velocity, test duration, test environment, and the effective mechanical stiffness of contact at the wear interface [17,18]. For a given wear test, these parameters

are effectively set, and care should be taken to avoid changes in any during a given experiment. In particular, changes in nominal contact stress and effective contact stiffness must be monitored, as these are likely to vary during the course of an experiment.

The solid contact which eventuates in a wear test gives rise to surface and subsurface material processing, both on the specimen and on the counterface. In large measure, the level of relative sliding velocity, together with specimen/counterface geometrical conformity, determine the heat generated at the wear interface. The thermal gradients associated with generation and dissipation of this heat are important both in physical and chemical processes which occur to create new specimen/counterface material "mixes" in situ. Figure 2 is useful in illustrating the form of subsurface structures developed in test materials during a typical wear experiment. In this figure, three characteristic zones are noted; Zone 1 is simply the unaffected base substrate. Zone 2 is a material region which shows evidence of plastic deformation, but which still consists wholly of base material. Zone 3 is compositionally distinct from the base material, and usually consists of material both from specimen and counterface. It is this Zone 3 material which results from the thermal and mechanical processing at and near the wear interface. The transport of material from specimen to counterface and vice versa is documented in recent work [8,9], but the precise mechanisms underlying such transfer depend upon particular materials and test conditions, and are not yet well understood.

Following a wear test of given duration, the specimen and counterface are evaluated for material attrition. Typically, this is in the form of a weight loss or volume change measurement, with volume change being a more generalizable

measure when comparisons between materials (of different densities) are being made. Beyond sheer volume of material removed, however, there are questions which arise pertaining to the processes and mechanisms by which particular materials wear under given experimental conditions. These are answered only through rather extensive analysis procedures, as depicted in Figure 1.

In such analysis, it is important to note that both specimen and counterface materials must be inspected, and with each of these both surface and subsurface examination is required for a complete description of a given wear process. In addition, the debris arising from these materials should also be examined. A variety of instrumental techniques is available for such analyses, including optical and scanning electron microscopy (SEM), as well as replica transmission electron microscopy (TEM), all of which yield micrographs which provide information on surfaces or on subsurface sections. In addition, the thin foil TEM technique can be employed to allow detailed examination of wafer-thin sections of material comprising various regions in the near-surface zones from specimen and/or counterface. Energy dispersive X-Ray (EDX) analysis represents another tool, particularly useful for documenting material transport in a global sense (over an entire specimen surface) or on a local, microscopic sense (examining Zone 3 for particular elements). X-Ray diffraction is useful also, particularly in the analysis of wear debris. By this means, particular chemical reaction products can be identified, having been produced in situ during wear. By this technique, phase transformations have been documented [8], and estimates concerning interfacial temperatures arising during solid contact have been made. Color metallography is another technique which has been utilized to document chemical reactions occurring during wear [12]. In this, particular oxides, known to form at specific temperatures, have been identified by virtue of characteristic colors. In addition to these techniques,

microhardness measurements can be performed on subsurface sections, in order to provide additional information concerning the properties of near-surface material zones produced in situ during a wear test [12]. Further still, profilometry can be employed either to obtain surface roughness information, or to obtain data on wear scar dimensions [13].

From the above descriptions of the large number of external variables operative in wear, and from the large number of analysis techniques which must be employed to obtain an adequate post-test characterization of specimen and counterface materials, it is not surprising that a holistic model of wear has not yet emerged. Thus, with the preceding as prologue, the report continues with an explication of recent experimental findings, followed by a section which presents results obtained in analysis.

Experimental

Both impulsive and steady sliding experiments have been conducted with various titanium alloys contacting stainless steel counterface materials [12]. In this, plastic strain measurements in Zone 2 reveal enormous deformations as shown in Figure 3. Moreover, significant variations in hardness have been documented in subsurface zones by microhardness measurements as indicated in Figure 4. Further, analysis of debris resulting from such materials under various experimental conditions reveals that particular reaction products are formed in response to specific "external variables", most notably relative sliding velocity. This behavior is illustrated in Table 1.

Additional work with titanium alloy pin specimens in steady sliding contact against steel counterface materials has demonstrated significant "stiffness" effects [17]. In essence, pins having different unsupported lengths were utilized as a means to obtain varying mechanical stiffness at the wear interface.

Figure 5 illustrates the different surface roughnesses obtained (R_a = centerline average across the lay direction measured over a 0.08 mm traverse) for pins varying in length (stiffness) at two levels of nominal contact stress. It is clear that contact stiffness is important in surface morphology, and this is further demonstrated in surface and subsurface micrographs [17]. Moreover, Figure 6 illustrates the "stiffness effect" in a "simple" steady sliding experiment. In this, it is apparent that material transport varies according to stiffness, and results depend also on the nominal contact stress level. Thus, both compositional and morphological features of the wear process depend upon a stiffness parameter which, until the present time, has not been recognized as relevant.

A similar and equally important "stiffness" effect has been established in the case of repetitive impulsive contact [18]. In this, the unsupported length of impacting 1410 steel (Fe-14Co-10Ni-2Cr-1Mo-0.16C) pins was varied to obtain varying stiffness in compound impact wear testing against stainless steel counterface materials. Figure 7 shows the vastly different wear track profiles obtained in otherwise identical wear tests which utilize pins of three different lengths. Figure 8 further documents the phenomenologically differing behavior obtained in this experimental series. Clearly, fundamentally distinct physical processes arise and produce unique material responses which depend upon the stiffness effect. These wear behaviors themselves can be analyzed by reference to subsurface observations and various characterization procedures as outlined in the Introduction.

Experiments designed to obtain measurements of temperatures arising under various experimental conditions are depicted in Figure 9. Both "internal" and "external" thermocouple junctions have been utilized to obtain data points for various conditions of compound impact wear. The "internal" measurements involve

forming the thermocouple junction on the "inner" surface of a titanium alloy cap. This cap is initially 1 mm in thickness, and becomes progressively thinner as wear occurs due to repetitive impact against a stainless steel counterface. For "external" measurements, the thermocouple junctions are formed at specific locations on the cylindrical surface of the specimen, at prescribed distances from the flat, impacting end. This end approaches the thermocouple locations as the wear test continues, so data are obtained as a function of position from the wear interface.

These experiments have not progressed to a final stage, as thermocouple response is inadequate for the short-lived transient effects known to occur during impulsive contact. Nonetheless, Figure 10 represents a conservative, "lower bound" on bulk temperatures occurring at various locations within a titanium alloy specimen (Ti-5Al-5Sn-2Zr-2Mo-0.25Si) in compound impact against a stainless steel counterface (Fe-17Cr-4Ni-4Cu) at 10 m/s at a nominal peak impulsive normal stress of 69 MPa. From these data, extrapolation to higher flash temperatures at asperity contacts underlines the significance of thermal phenomena in high speed sliding contact. In particular, high temperatures and strong thermal gradients will promote diffusion of specimen into counterface (in Zone 3), and vice versa. This, together with mechanical mixing associated with adhesive and abrasive mechanisms, creates a near-surface microstructure which is unique and dependent upon test materials and conditions. The Zone 3 adjoins Zone 2 which is extremely plastically deformed, and which often shows a refinement in structure near the Zone 2/Zone 3 interface. The particular subsurface zone structure which does develop in a given wear test is established quickly, and tends to persist in a state of dynamic equilibrium [15]. In this process, it appears that Zone 3 is replenished both from Zone 2 and from the counterface material. Clearly, the properties of such in situ

zones and the nature of the bonds between Zones 2 and 3 are significant in terms of material attrition.

Analytical

The overall objective of the analysis has been the description of the state of stress and strain in a cylindrical wear test specimen repetitively impacted against a moving rough counterface plane. In this work, the authors first assessed quantitatively the influence of the dynamic processes on the stress level in the specimen. This was achieved by modeling the specimen as a rod impacting, in a controlled way, an elastic half-space. The detailed description of this part of the analysis was given both in previous reports [1,2] as well as in the technical literature [19-20]. As reported, the numerical results confirmed the intuitive expectation that the flexibility of the half-space has a moderating influence on both displacements and stresses.

This analysis also has shown that for the relatively low approach velocities associated with present experiments in impact wear, the dynamic effects are of secondary importance. Therefore, in subsequent work, the emphasis has been placed on the solution of a quasi-static state of stress and strain (inertia effects neglected) in a finite circular cylinder pressed against a rough moving rigid plane. This problem has been described in earlier reports [2,3]. However, in the period following the last Scientific Report [3], considerable changes in the analysis were made. This warrants a revision of the earlier formulation in addition to the discussion of final findings.

Although the problem is relatively simple both geometrically and physically, it presents considerable mathematical difficulty. Presumably, this is why none of the known analyses of circular cylinders have dealt with a non-axisymmetric case as presented here. Indeed, stresses and strains in

an elastic, circular cylinder were first discussed by Pochhammer [21] and Chree [22]. Later Filon [23] published the solutions to several cylinder problems. Both Chree and Filon pointed out the difficulty involved in satisfying simultaneously the boundary conditions on the stress-free lateral surface and on the flat ends of the cylinder. In fact, the conditions at the ends were satisfied only approximately. One of the axisymmetric problems considered by Filon -- that of a right circular cylinder pressed between two rough, rigid plates -- was re-examined by Pickett [24] who succeeded in satisfying the boundary conditions on both the lateral surface and the flat ends. Indeed, this work has shown that the shear stresses at the flat ends of the cylinder are singular at the edges. The specific type of the singularity, however, was not determined. This was achieved only recently by Benthem and Minderhoud [25]. These authors also investigated only an axially symmetric problem, but used the method of radial eigenfunction expansion presented by Little and Childs [26]. The strength of the singularity of the shear stress at the edge of the flat end, with zero in-plane displacements, was found in [25] as the solution of a particular, eigenvalue problem. In this, the results show that the index of the strength depends on the Poisson's ratio. Indeed, the numerical results obtained in [25] apply to any semi-infinite or finite, circular cylinder with flat end fixed and the other end subjected to uniform pressure. Thus, this work [25] represents the first satisfactory solution for the solid cylinder compressed in an axially symmetric manner between rough rigid stamps.

In later analysis, Gupta [27] solved a similar problem, and used an ingenious, alternate method of determining the strength of the singularity and the stress intensity factor. The results in [27] confirmed the correctness of the results obtained in [25]. Now, in the present analysis, the diffi-

culties encountered in [25] and [27] are amplified by several factors, including (1) lack of axial symmetry; and (2) more complicated boundary conditions at the end subjected to frictional tractive forces generated by the contact with the moving rigid counterface plane.

The three-dimensional problem of the theory of elasticity considered in the present analysis involves solving the Navier equations, i.e., a set of coupled, partial differential equations in unknown displacements (Eqs. 1)*. Partial uncoupling of these equations was achieved by expressing the displacements in terms of the Papkovich-Neuber potentials, (Eqs. 2). This technique, however, complicates the boundary conditions.

Consequently, the symmetry of the cylinder with respect to one of the longitudinal sections was utilized (Figure 11) to define the types of integral transforms appropriate for the present case (Eqs. 8) [Note these differ from those of [2] and [3]]. Subsequent elimination of the axial and angular variables was achieved by means of application of double finite Fourier transformations to both the differential equations and the boundary conditions, (Eqs. 7, 11). In this process, the shear stresses at the flat ends appear as the basic unknowns of the problem (Eqs. 10).

Finally, utilization of the transformed boundary conditions at the flat ends (Eqs. 5, 6) leads to a coupled infinite system of singular integral equations (Eqs. 12) defining the unknown Fourier coefficients (which are still functions of the radial variable) of the shear stresses at the flat ends.

Then, the method of collocation was chosen as the technique suitable to obtain the numerical solution of the system.

The first part of the analysis involved considerable conceptual and algebraic difficulties. This was true also in the numerical work. Firstly,

* The basic equations are given in the Appendix.

it was necessary to represent the unknown function corresponding to the radial component of the shear stress at the fixed flat end as the sum. This was comprised of a singular function (with the singular part known from [25]), and a regular part which was put in the form of a trigonometric series (Eq. 14). Secondly, some of the kernels were in the form of slowly convergent infinite series. Therefore, asymptotic expressions had to be derived which were valid for a large index of summation. This process allowed kernels to be represented in the form of a finite series and a closed form function (Eq. 13). Thirdly, most kernels exhibit Cauchy type singularities for $r = \rho$ (r and ρ being the arguments of the kernels). Finally, as is well known, choice of the location of the collocation points is of importance.

Because of the accumulation of so many complications, it was felt that it is important to have some objective tests of the numerical results. Several such tests were devised and utilized, as follows:

1) For the friction coefficient, k, equal to zero, the description of the present problem reduces to a single integral equation. This corresponds to the axisymmetric problem solved in [25]. The comparison of the shear stresses for the selected case $\nu = .25$ and the length of the cylinder being equal to its diameter are presented in Table 2. It should be noted that in order to make both the present results and the results from [25] comparable, a simple adjustment has been made (in [25] the normal stress at the far end is assumed to be uniform; here-- the normal displacement is uniform). By the de Saint Venant principle, both cases should lead to the same results at distances sufficiently removed from the far end).

As seen from Table 2, the correlation of results is very good, including those obtained for the stress concentration factor. Figure 12 gives the normal stresses at the interface between the cylinder and the rigid plate.

2) For the friction coefficient $k \neq 0$, one expects that the behavior of a sufficiently slender cylinder will be similar to a cantilever with zero slope at the free end (Fig. 13). The equation for the displacement of the beam from Fig. 13 was derived (Eqs. 15, 16), and the corresponding displacement of the cylinder calculated for various values of k showing very good agreement. Also, the normal stress distribution for $k \neq 0$ is qualitatively similar (except for the singularities present here) to the stress distribution resulting from simple beam theory. Table 3 gives the numerical values of shear and normal stresses at both flat ends and Table 4 the variation of the stress concentration factor with the angle θ for the case $k = .15$, $\nu = .25$, and the length to diameter ratio equal to 1. Graphical results for those quantities are presented in Fig. 14.

3) Since the regular parts of the unknown functions are in form of cosine series, one would expect that an increase in the number of the collocation points should lead to a converging sequence of values for each of the coefficients of the series. Ultimately, these coefficients should equal the Fourier coefficients of the corresponding function. The known limitations of the collocation method, however, did not permit an arbitrary increase in the number of the collocation points. Still, the trend toward convergence is clearly visible. In fact, the first few coefficients converge when the number of the collocation points is 7.

Thus, the analytical work [28,29] has contributed to the understanding of the mechanical behavior of a cylindrical specimen subjected to frictional and normal forces at the free end (the wear interface). These results constitute the groundwork for a truly dynamical analysis which also was initiated in the present project (see [3] for description). Further, the analysis presents

the starting point for taking into account the plastic phenomena observed in the laboratory tests. Thus, the analysis of subsurface zone formation for given materials and experimental conditions remains for future work.

Acknowledgement

The authors are grateful for the contributions of Research Assistant Steven F. Wayne and Graduate Assistant Rhoby J. Conant.

References

[1] Rice, S. L. and Solecki, R., "Wear of Homogeneous and Composite Materials under Conditions of Repeated Normal and Sliding Impact." AFOSR-TR-77-0857, 1977.

[2] Rice, S. L. and Solecki, R., "Wear of Homogeneous and Composite Materials under Conditions of Repeated Normal and Sliding Impact: II." AFOSR-TR-78, 1978.

[3] Rice, S. L. and Solecki, R., "Wear of Homogeneous and Composite Materials under Conditions of Repeated Normal and Sliding Impact." AFOSR-TR-79-1241, 1979.

[4] Rice, S. L., "Reciprocating Impact Wear Testing Apparatus," Wear, 45, pp. 85-95. 1977.

[5] Rice, S. L., "A Review of Wear Mechanisms and Related Topics," Proc. Intl. Conf. on Fundamentals of Tribology, pp. 469-476. 1978.

[6] Rice, S. L., "The Role of Microstructure in the Impact Wear of Two Aluminum Alloys," Wear, 54, 2, pp. 291-301. 1979.

[7] Rice, S. L. and Wayne, S. F., "Wear of Two Titanium Alloys under Repetitive Compound Impact," Wear, 61, pp. 69-76. 1980.

[8] Rice, S. L., Nowotny, H. and Wayne, S. F., "Application of Material Transport Methodology to the Impact Wear of Two In-Situ Composites," Materials Science and Engineering, 45, 3, pp. 229-236. 1980.

[9] Rice, S. L., Wayne, S. F., Nowotny, H., "The Role of Material Transport in the Impact Wear of Titanium Alloys," to be published in Wear.

[10] Rice, S. L., "Variations in Wear Resistance Due to Microstructural Condition in High Strength Steel under Repetitive Impact," Tribology Intl., 12, 1, pp. 25-29, 1979.

[11] Nowotny, H., Rice, S. L. and Wayne, S. F., "Characteristics of Wear Debris in Impact Sliding," to be published in Wear.

[12] Wayne, S. F., Nowotny, H. and Rice, S. L., "Wear of Titanium Alloys under Repetitive Impulsive Loading," Proc. Fourth Intl. Conf. on Titanium, 1980.

[13] Rice, S. L., "Impact Wear of Graphite Epoxy Composites," Proc. 2nd Intl. Conf. on Solid Lubrication, ASLE, 1978.

[14] Rice, S. L., Nowotny, H. and Wayne, S. F., "Characteristics of Metallic Subsurface Zones in Sliding and Impact Wear," to be published.

[15] Rice, S. L., Nowotny, H. and Wayne, S. F., "Formation of Subsurface Zones in Impact Wear," ASLE No. 80-AM-2D. 1980.

[16] Rice, S. L., Nowotny, H. and Wayne, S. F., "Research Needs and Developments on Wear of Materials," Proc. VI InterAmerican Conf. on Materials Technology, ASME, 1980.

[17] Rice, S. L., Wayne, S. F. and Nowotny, H., "The Role of Specimen Stiffness in Sliding Wear," to be published.

[18] Rice, S. L., Wayne, S. F. and Nowotny, H., "The Role of Specimen Stiffness in Impact Wear," to be published.

[19] Solecki, R., "Controlled Impact of a Finite, Elastic, One-dimensional Rod upon an Isotropic, Elastic Half-space, Proc. 7th Canadian Congress of Applied Mechanics, Sherbrooke, Canada, May 27-June 1, pp. 266-267. 1979.

[20] Solecki, R.,"Controlled Impact of a Finite, Elastic, Circular Rod on an Isotropic Elastic Half-space," J. Acoust. Soc. Am. 66, 2, pp. 509-513. 1979.

[21] Pochhammer, L., uber die Fortpflanzungsgeschwindigkeiten Kleiner Schwingungen in Einem Unbegrenzten Isotropen Kreiszylinder, J. reine angew. Math. (Crelle's J.) 81, pp. 324-336, 1876.

[22] Chree, C., "The Equations of an Isotropic Elastic Solid in Polar and Cylindrical Coordinates, Their Solutions and Applications," Trans. Cambridge Phil. Soc., 14, 1889, pp. 250-369.

[23] Filon, L. G., "The Elastic Equilibrium of Circular Cylinders under Certain Practical Systems of Load," Phil. Trans. Roy. Soc., Series A, 198, pp. 147-233, 1902.

[24] Pickett, G., "Application of the Fourier Method to the Solution of Certain Boundary Value Problems in the Theory of Elasticity," J. Appl. Mech., 11, pp. 167-183, 1944.

[25] Benthem, J. P., Minderhoud, P., "The Problem of the Solid Cylinder Compressed Between Rough Rigid Stamps," Int. J. Solids Struct., 8, pp. 1027-1042. 1972.

[26] Little, R. W., Childs, S. B., "Elastostatic Boundary Region Problems in Solid Cylinders," Q. Appl. Math., 25, pp. 261-274. 1967.

[27] Gupta, G. D., "The Analysis of the Semi-infinite Cylinder Problem," Int. J. Solids Struct., 10, pp. 137-148. 1974.

[28] Conant, R. J., Solecki, R., "The Effects of Sliding Friction on the Stresses and Deformations of an Elastic, Solid, Right Circular Cylinder Pressed Against a Rough Rigid Surface", to be published.

[29] Conant, R. J., Solecki, R., "Axisymmetric Compression of the Finite Elastic Cylinder with One End Fixed", to be published.

Table 1 Wear Debris Analysis* After Impact Sliding by X-ray Powder Diagrams (counterface 17-4 PH Steel).

Specimen Material	Relative Transverse Sliding Velocity (m/s)						
	0.01	0.1	1.0	2.1	4.2	6.3	10.0
5522S (α,β)	**α-Fe** / **α-Ti**	**α-Fe** / **α-Ti**	**α-Fe** / **α-Ti**	**α-Fe** / **α-Ti** / α-Fe_2O_3	**α-Fe** / **α-Ti** / αFe_2O_3	**α-Fe** / **γ-Fe** / αFe_2O_3	**α-Fe** / **γ-Fe** / αFe_2O_3 / α-Ti
Beta (β)		**α-Fe** / **β-Ti**	**α-Fe** / **β-Ti**	**α-Fe** / **β-Ti** / γ-Fe / αFe_2O_3	**α-Fe** / **β-Ti** / αFe_2O_3 / γ-Fe	**α-Fe** / **β-Ti** / αFe_2O_3	**β-Ti** / **α-Fe** / γ-Fe
Ti_3Al		**Ti_3Al** / α-Fe					**α-Fe** / **γ-Fe** / αFe_2O_3 / Ti_3Al
IMI 685				**α-Fe** / **α-Ti** / αFe_2O_3	**α-Fe** / **α-Ti** / αFe_2O_3		

*underlined = major amount

Table 2

Values of $G_{20}(\rho) = a_1 f_\infty(\rho) + \sum_{i=2}^{N} a_1 \cos \frac{(i-2)\pi\rho}{\tau}$ for $\tau = 0.5$, $\nu = .25$, $\lambda = .25525$

1	2	3	4	5
Coll. point ρ	G_{20}	Selected values of ρ	G_{20} (lin. interp. of column 2)	Converted G_{20} from [25] for 11 unknowns.
.00	.0000	.00	.0000	.0000
.02	.0061	.10	.0311	.0295
.05	.0153	.20	.0650	.0674
.075	.0231	.30	.1054	.1021
.10	.0311	.40	.1643	.1687
.14	.0441	.45	.2201	.2144
.18	.0577			
.22	.0723			
.26	.0880			
.30	.1054			
.34	.1253			
.38	.1490			
.42	.1796			
.44	.1998			
.47	.2464			

Stress concentration factor

(a) Present study = .09770

(b) Converted value from [25] = .09783

NOTES: $\rho = 0$ is located at the center and $\rho = .5$ at the edge of the cross-section of the cylinder.

Conversion factor K_1 used to multiply values from [25] to obtain G_{20}.

$$K_1 = \frac{\sigma_{av}}{2(1-\nu)} = 0.8487$$

Conversion factor K_2 used to multiply the value of the stress concentration factor from [25]:

$$K_2 = \frac{\sigma_{av}(\tau)^\lambda}{2(1-\nu)} = 0.7094$$

where σ_{av} obtained here for 14 collocation points is 1.273.

Table 3

Stresses at the flat ends for $\tau = 0.5$, $\nu = .25$, $\lambda = .25525$, $k = 0.15$, 8 Fourier coefficients.

Coll. points	$\theta=0°$ σ_{zz} at $z = 0$	$\theta=90°$ σ_{zz} at $z = 0$	$\theta=180°$ σ_{zz} at $z = 0$	$\theta=0°$ σ_{zz} at $z = \ell$	$\theta=90°$ σ_{zz} at $z = \ell$	$\theta=180°$ σ_{zz} at $z = \ell$	$\theta=0°$ σ_{xz} at $z = \ell$	$\theta=90°$ σ_{xz} at $z = \ell$	$\theta=180°$ σ_{xz} at $z = \ell$
.10	-1.214	-1.262	-1.299	-1.213	-1.130	-1.046	-0.236	-0.197	-0.1417
.20	-1.075	-1.258	-1.448	-1.304	-1.133	-0.963	-0.291	-0.195	-0.0970
.30	-0.975	-1.260	-1.564	-1.505	-1.205	-0.905	-0.394	-0.184	-0.0277
.40	-0.763	-1.245	-1.797	-1.710	-1.206	-0.708	-0.437	-0.170	0.0533
.45	-0.614	-1.240	-2.035	-2.028	-1.324	-0.631	-0.544	-0.152	0.0954
.47	-0.600	-1.236	-2.144	-2.218	-1.452	-0.711	-0.615	-0.138	0.1292

Table 4

Variation of the stress concentration factor with the angle for $k = 0.15$, $\tau = 0.5$, $\nu = .25$, $\lambda = .75525$, 8 Fourier coefficients.

Stress concentration factor				
$\theta = 0°$	$\theta = 45°$	$\theta = 90°$	$\theta = 135°$	$\theta = 180°$
0.1114	0.1047	0.0954	0.0866	0.0842

Appendix. The Effects of Sliding Friction on the Stresses and Deformations of an Elastic, Solid, Right Circular Cylinder Pressed Against a Rough Rigid Surface.

Basic Equations (they replace the equations given in the Appendix to the report [2]).

Navier equations in cylindrical coordinate system

$$\nabla^2 u_r - \frac{u_r}{r^2} - \frac{2}{r^2}\frac{\partial u_\theta}{\partial \theta} + \frac{1}{1-2\nu}\frac{\partial \Delta}{\partial r} = 0$$

$$\nabla^2 u_\theta - \frac{u_\theta}{r^2} + \frac{2}{r^2}\frac{\partial u_r}{\partial \theta} + \frac{1}{1-2\nu}\frac{1}{r}\frac{\partial \Delta}{\partial \theta} = 0$$

$$\nabla^2 u_z + \frac{1}{1-2\nu}\frac{\partial \Delta}{\partial z} = 0 \qquad (1)$$

where u_r, u_θ, u_z are the physical components of the displacement vector $\underline{u}$ and where ∇^2 is the Laplacian and Δ the dilatation

$$\nabla^2 = \frac{\partial^2}{\partial r^2} + \frac{1}{r}\frac{\partial}{\partial r} + \frac{1}{r^2}\frac{\partial^2}{\partial \theta^2} + \frac{\partial^2}{\partial z^2}$$

$$\Delta = \frac{\partial u_r}{\partial r} + \frac{1}{r}\left(\frac{\partial u_\theta}{\partial \theta} + u_r\right) + \frac{\partial u_z}{\partial z}$$

Papkovich-Neuber substitution (where Ψ_z is assumed equal zero)

$$u_r = \frac{\partial}{\partial r}(\phi + r\Psi_r) - 4(1-\nu)\Psi_r$$

$$u_\theta = \frac{\partial}{r\partial \theta}(\phi + r\Psi_r) - 4(1-\nu)\Psi_\theta$$

$$u_z = \frac{\partial}{\partial z}(\phi + r\Psi_r) \qquad (2)$$

leads to the partial uncoupling of eq. (1) in the form:

$$\nabla^2 \Psi_r - \frac{2}{r^2} \frac{\partial \Psi_\theta}{\partial \theta} - \frac{1}{r^2} \Psi_r = 0$$

$$\nabla^2 \Psi_\theta + \frac{2}{r^2} \frac{\partial \Psi_r}{\partial \theta} - \frac{1}{r^2} \Psi_\theta = 0$$

$$\nabla^2 \phi = 0 \qquad (3)$$

Boundary conditions at the lateral surface

$$\sigma_{rr} = \frac{1-\nu}{(1+\nu)(1-2\nu)} E \left[4(1-\nu) \frac{\partial \Psi_r}{\partial r} - \frac{\partial^2}{\partial r^2} (\phi + r\Psi_r)\right] + \frac{E}{2(1+\nu)} \left[\frac{4(1-\nu)}{r} \frac{\partial \Psi}{\partial \theta}\right.$$

$$\left. - \frac{1}{r^2} \frac{\partial^2}{\partial \theta^2} (\phi + r\Psi_r) + \frac{4(1-\nu)}{r} \Psi_r - \frac{1}{r} \frac{\partial}{\partial r} (\phi + r\Psi_r) - \frac{\partial^2}{\partial z^2} (\phi + r\Psi_r)\right] = 0$$

$$\sigma_{rz} = \frac{E}{1+\nu} \left[2(1-\nu) \frac{\partial \Psi_r}{\partial z} - \frac{\partial^2}{\partial r \partial z} (\phi + r\Psi_r)\right] = 0$$

$$\sigma_{r\theta} = \left[\frac{4(1-\nu)}{r} \frac{\partial \Psi_r}{\partial \theta} - \frac{2}{r} \frac{\partial^2}{\partial r \partial \theta} (\phi + r\Psi_r) - \frac{4(1-\nu)}{r} \Psi_\theta + \frac{2}{r^2} \frac{\partial}{\partial \theta} (\phi + r\Psi_r)\right.$$

$$\left. + 4(1-\nu) \frac{\partial \Psi_\theta}{\partial r}\right] \frac{E}{1+\nu} = 0 \qquad (4)$$

Boundary conditions at $z=\ell$ (fixed end)

$$u_r = \frac{\partial}{\partial r} (\phi + r\Psi_r) - 4(1-\nu) \Psi_r = 0$$

$$u_\theta = \frac{1}{r} \frac{\partial}{\partial \theta} (\phi + r\Psi_r) - 4(1-\nu)\Psi_\theta = 0$$

$$u_z = \frac{\partial}{\partial z} (\phi + r\Psi_r) = W \qquad (5)$$

Boundary conditions at z=0 (the interface)

$$u_z = \frac{\partial}{\partial z}(\phi + r\Psi_r) = 0$$

$$\sigma_{\theta z} = -k\sigma_{zz} \sin\theta \quad \text{or}$$

$$\frac{E}{2(1+\nu)}\left[\frac{\partial^2}{r\partial\theta\partial z}(\phi + r\Psi_r) - 4(1-\nu)\frac{\partial \Psi_\theta}{\partial z}\right] + k \sin\theta\left\{\frac{3-2\nu}{2(1+\nu)(1-2\nu)} E\right.$$

$$\left.\left[\frac{\partial^2}{\partial z^2}(\phi + r\Psi_r)\right] - \frac{E}{1+\nu}(1-2\nu)\frac{1}{r}\left[\frac{\partial}{\partial r}(r\Psi_r) + \frac{\partial \Psi_\theta}{\partial \theta}\right]\right\} = 0$$

$$\sigma_{rz} = k\,\sigma_{zz} \cos\theta \qquad (6)$$

Fourier transforms with respect to θ and z of the field equations (3) yields:

$$L_1\bar{\Psi}_r + \frac{2n}{r^2}\bar{\Psi}_\theta = G_{1n}(r) - (-1)^m G_{2n}(r) \qquad m = 0,1,\ldots,\ n = 0,1,\ldots$$

$$L_1\bar{\Psi}_\theta + \frac{2n}{r}\bar{\Psi}_r = G_{3n}(r) - (-1)^m G_{4n}(r) \qquad m = 0,1,\ldots,\ n = 1,2,\ldots$$

$$L_2\bar{\Phi} = -r[G_{1n}(r) - (-1)^m G_{2n}(r)] \qquad m = 0,1,\ldots,\ n = 0,1,\ldots$$

(7)

where

$$\bar{\Psi}_r(r,n,m) = \int_0^{\ell}\int_0^{\pi} \Psi_r(r,\theta,z) \cos n\theta \cos\lambda_m z\, d\theta dz$$

$$\bar{\Psi}_\theta(r,n,m) = \int_0^{\ell}\int_0^{\pi} \Psi_\theta(r,\theta,z) \sin n\theta \cos\lambda_m z\, d\theta dz$$

$$\bar{\phi}(r,n,m) = \int_0^{\ell}\int_0^{\pi} \phi(r,\theta,z) \cos n\theta \cos\lambda_m z\, d\theta dz \qquad (8)$$

where

$$L_1 = \frac{d^2}{dr^2} + \frac{1}{r}\frac{d}{dr} - \frac{n^2+1}{r^2} - \lambda_m^2 \qquad L_2 = \frac{d^2}{dr^2} + \frac{1}{r}\frac{d}{dr} - \frac{n^2}{r^2} - \lambda_m^2$$

(9)

and where the basic unknowns $G_{1n}(r)$, $G_{2n}(r)$, etc. are proportional to the Fourier transforms of the shear stresses at the ends:

$$G_{1n}(r) = \frac{1+\nu}{2E(1-\nu)} \int_0^{\pi} \sigma_{rz}(r,\theta,z=0) \cos n\theta d\theta , \qquad n = 0,1,...$$

$$G_{2n}(r) = \frac{1+\nu}{2E(1-\nu)} \int_0^{\pi} \sigma_{rz}(r,\theta,z=\ell)\cos n\theta \, d\theta , \qquad n = 0,1,...$$

$$G_{3n}(r) = \frac{1+\nu}{2E(1-\nu)} \int_0^{\pi} \sigma_{\theta z}(r,\theta,z=0)\sin n\theta \, d\theta , \qquad n = 1,2,...$$

$$G_{4n}(r) = \frac{1+\nu}{2E(1-\nu)} \int_0^{\pi} \sigma_{\theta z}(r,\theta,z=\ell)\sin n\theta \, d\theta , \qquad n = 1,2,...$$

(10)

Fourier transforms of the boundary conditions at the lateral surface

$$(5-12\nu + 8\nu^2)\frac{d\bar{\Psi}_r}{dr} + [-\lambda_m^2 R^2 - (n^2+1) + 2(1-2\nu)^2]\frac{1}{R}\bar{\Psi}_r + 8n\nu(1-\nu)\frac{1}{R}\bar{\Psi}_\theta -$$

$$(\frac{n^2}{R^2} + \lambda_m^2)\bar{\Phi} + \frac{1}{R}\frac{d\bar{\Phi}}{dr} = 2(1-\nu)\, R[G_{1n}(R) - (-1)^m G_{2n}(R)]$$

$$(1-2\nu)\bar{\Psi}_r - \frac{d\bar{\Phi}}{dr} - R\frac{d\bar{\Psi}_r}{dr} = 0$$

$$\frac{n}{R}\bar{\Psi}_r + \frac{n}{R^2}\bar{\Phi} - 2(1-\nu)\frac{\bar{\Psi}_\theta}{R} + 2(1-\nu)\frac{d\bar{\Psi}_\theta}{dr} = 0$$

(11)

Sample equations from the resulting system of singular integral equations:

n=0:

$$\int_0^\tau G_{10}(\xi)K_1(\rho,\xi)d\xi + \int_0^\tau G_{20}(\xi)K_2(\rho,\xi)d\xi = -\nu\pi\,\hat{W}\rho$$

$$2(1-\nu)\,[G_{11}(\rho) - G_{31}(\rho)] + \int_0^\tau G_{10}(\xi)K_{19}(\rho,\xi)d\xi + \int_0^\tau G_{20}(\xi)K_{20}(\rho,\xi)d\xi =$$

$$(1+\nu)\pi k\hat{W}$$

n=1:

$$G_{10}(\rho) - G_{12}(\rho) + G_{32}(\rho) = 0$$

etc.

n=2,3,...∞ :

$$G_{1,n-1}(\rho) + G_{3,n-1}(\rho) - G_{1,n+1}(\rho) + G_{3,n+1}(\rho) = 0$$

$$\int_0^\tau G_{1n}(\xi)K_{11,n}(\rho,\xi)d\xi + \int_0^\tau G_{2n}(\xi)K_{12,n}(\rho,\xi)d\xi + \int_0^\tau G_{3n}(\xi)K_{13,n}(\rho,\xi)d\xi$$

$$+ \int_0^\tau G_{4n}(\xi)K_{14,n}(\rho,\xi)d\xi = 0 \qquad (12)$$

etc.

where $\tau = R/\ell$, $\rho = r/\ell$, $\hat{W} = W/\ell$.

The kernels $K_i(\rho,\xi)$ are represented by infinite series with very complicated general terms $\Phi_m(\rho,\xi)$ depending on various combinations of modified Bessel functions.

The kernels $K_i(\rho,\xi)$ were represented asymptotically, to improve convergence, in the form

$$K_i(\rho,\xi) \equiv \sum_{m=1}^{\infty} \phi_{m,i}(\rho,\xi) = f_i(\rho,\xi) + \sum_{m=1}^{M-1} [\phi_{m,i}(\rho,\xi) - \hat{\phi}_{m,i}(\rho,\xi)] \qquad (13)$$

where the functions $f_i(\rho,\xi)$ depend on hyperbolic functions and on logarithms.

Representation of the singular function $G_{2n}(\rho)$ used for the collocation method:

$$G_{2n}(\rho) = a_{1n}[(\tau-\rho)^{-\lambda} - (\tau-\rho)^{-1-\lambda} - \frac{1}{2}\lambda(\lambda+1)\rho\ (\rho-\tau)] + \sum_{i=2}^{N} a_{i,n} \cos\frac{(i-2)\pi\rho}{\tau} \qquad (14)$$

where N is the number of collocation points and where for $\nu = .25$, $\lambda = .25525$.

The horizontal displacement of the "rolling" end of the cantilever beam:

$$u_B = \frac{kR}{2\sqrt{w_0/\ell}} \frac{2(1-\cos\beta\ell) - \beta\ell\sin\beta\ell}{\sin\beta\ell} \qquad (15)$$

where $\beta = 2\frac{\ell}{R}\sqrt{\frac{w_0}{\ell}}$

For small $\beta\ell$:

$$u_B \approx \frac{kR\,(\beta\ell)^3}{24\sqrt{w_0/\ell}} \qquad (16)$$

METHODOLOGY USED IN IMPACT WEAR STUDIES

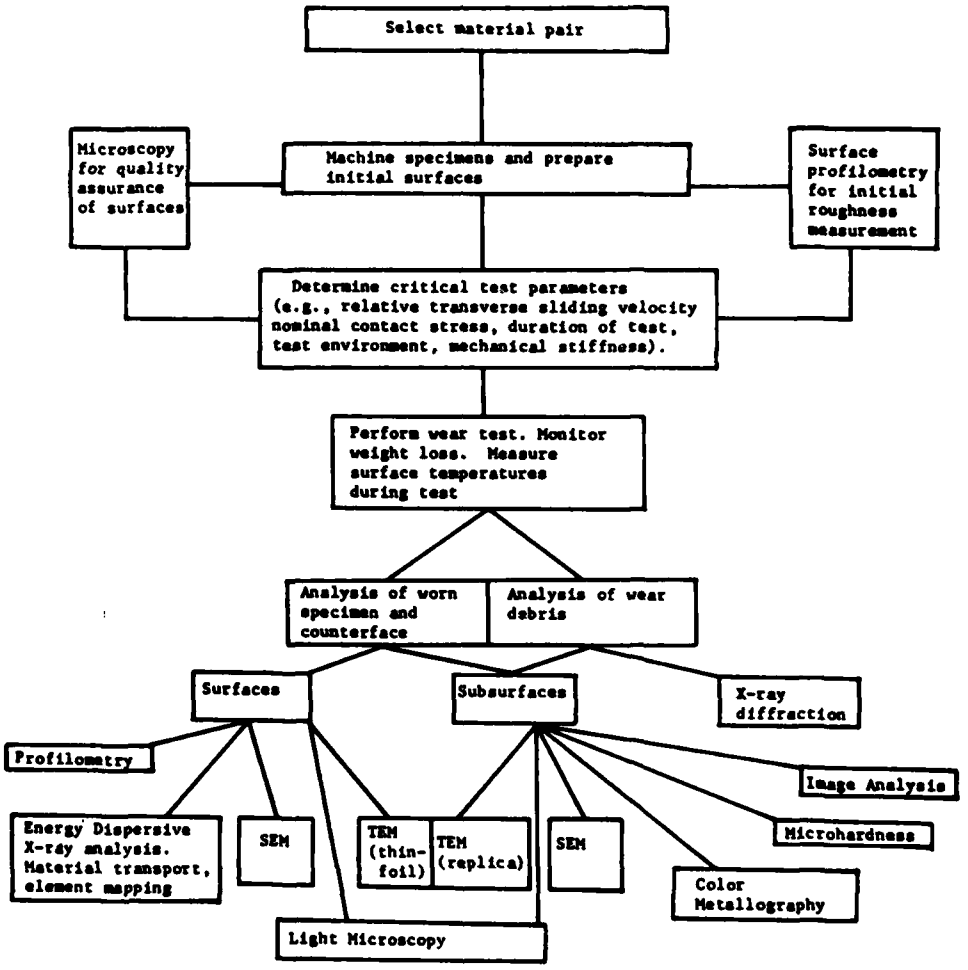

Fig. 1

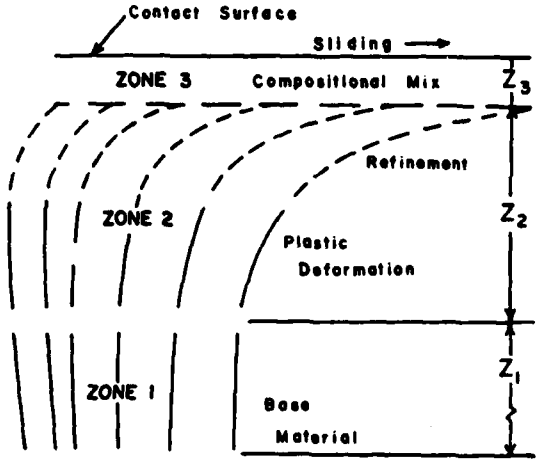
Contact Surface
Sliding
ZONE 3
Compositional Mix
Z_3
Refinement
ZONE 2
Z_2
Plastic
Deformation
Z_1
ZONE 1
Base
Material

Fig. 2

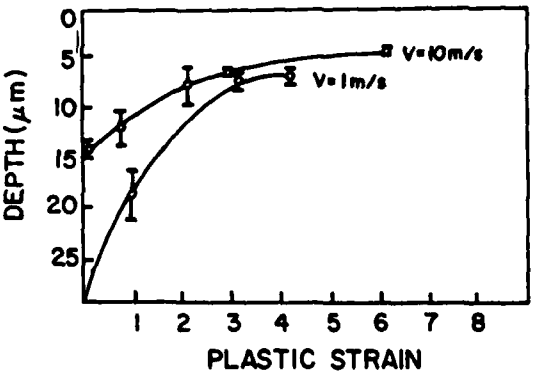
DEPTH (μm)
0
5
10
15
20
25
V=10m/s
V=1m/s
1
2
3
4
5
6
7
8
PLASTIC STRAIN

Fig. 3

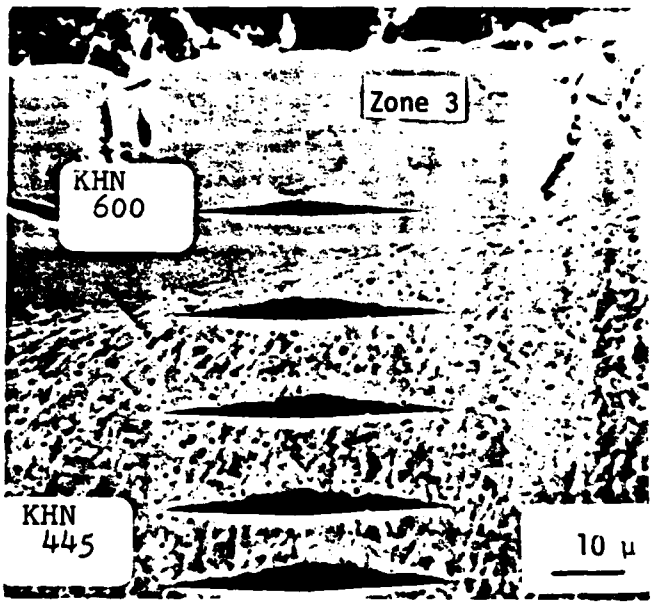

Figure 4 - Microhardness indentations beneath worn surface

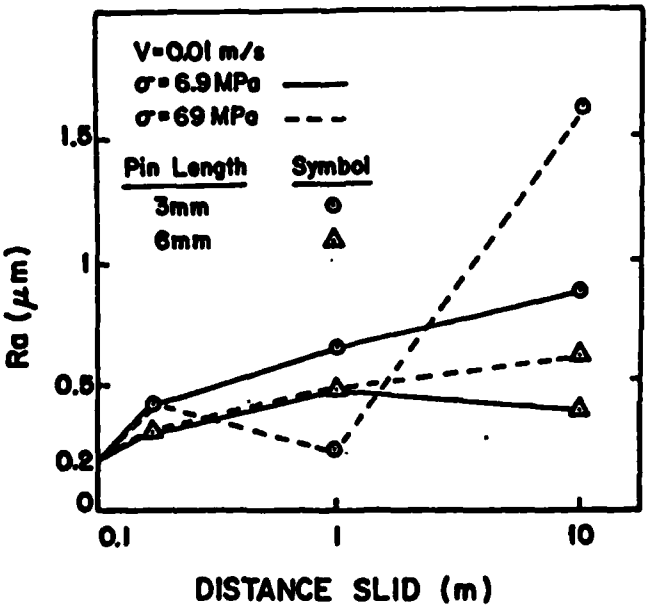

Fig. 5

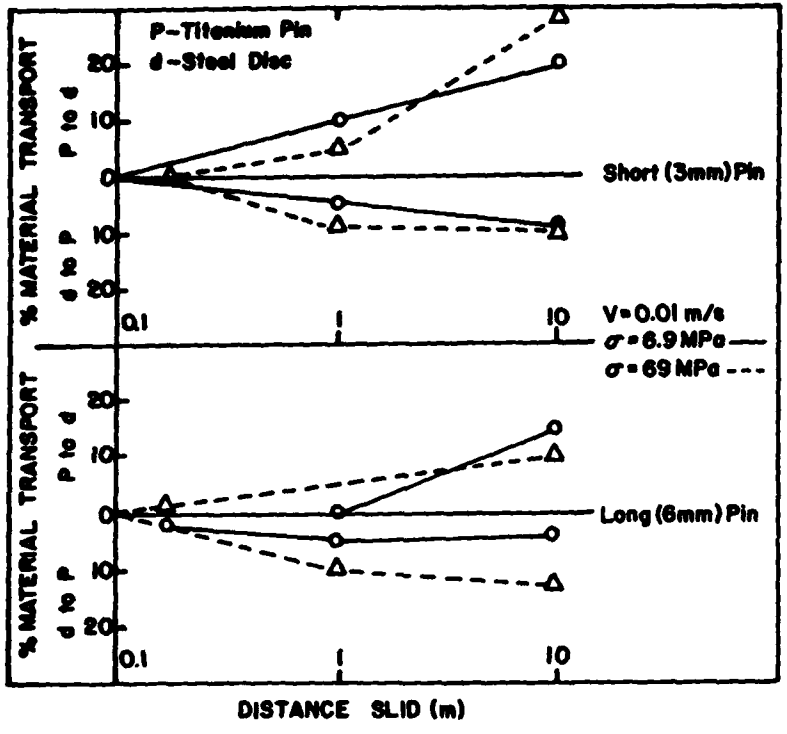

Fig. 6

WEAR TRACK PROFILES PRODUCED IN 17-4 COUNTERFACE BY 1410 PINS OF DIFFERING LENGTH

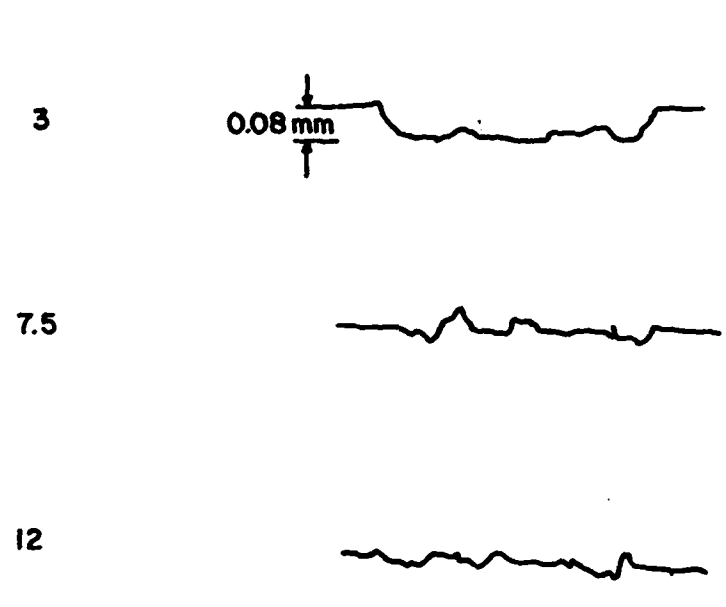

Fig.7

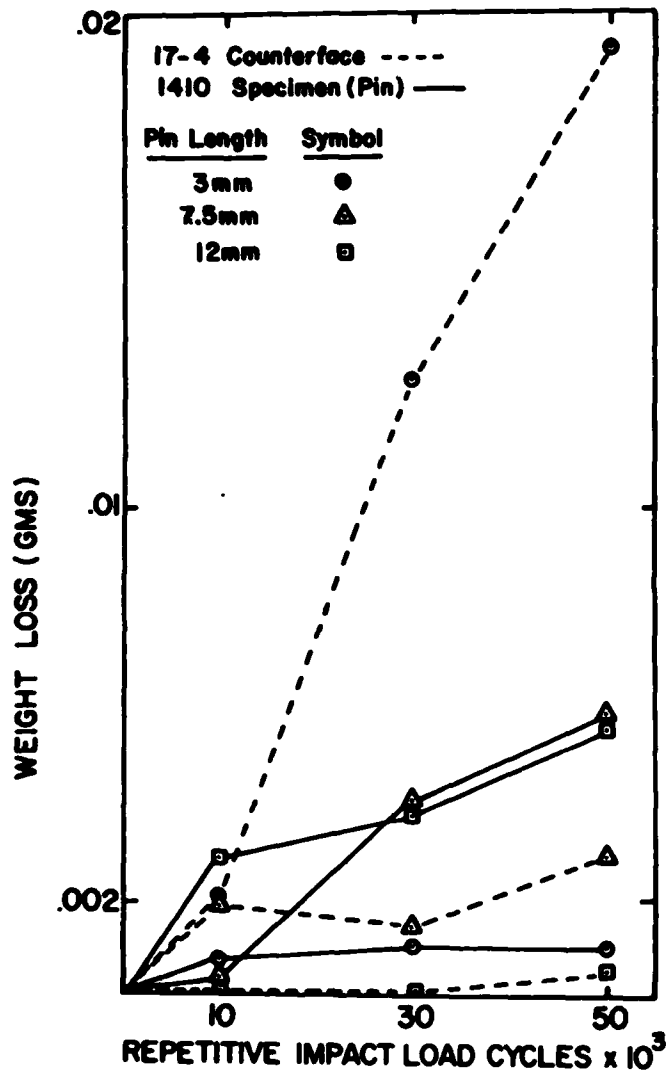

Fig. 8

TEMPERATURE MEASUREMENT

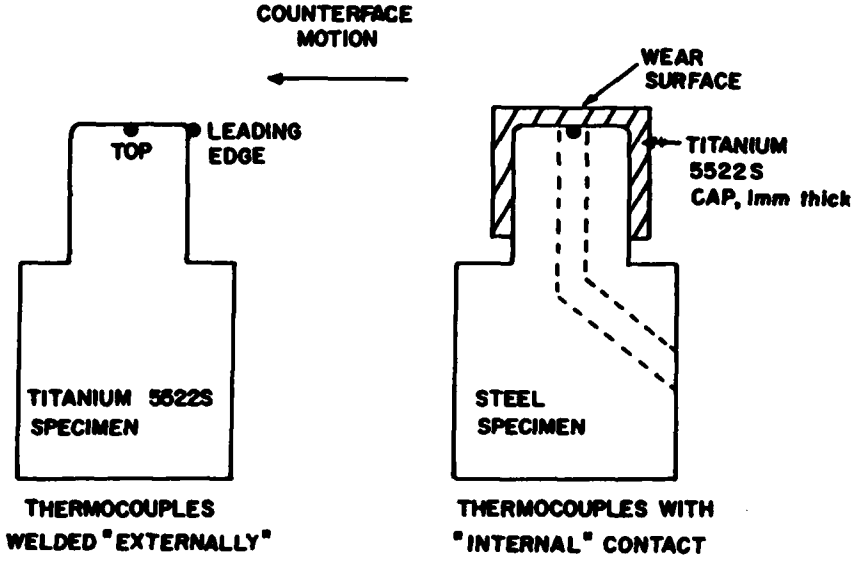

Fig. 9

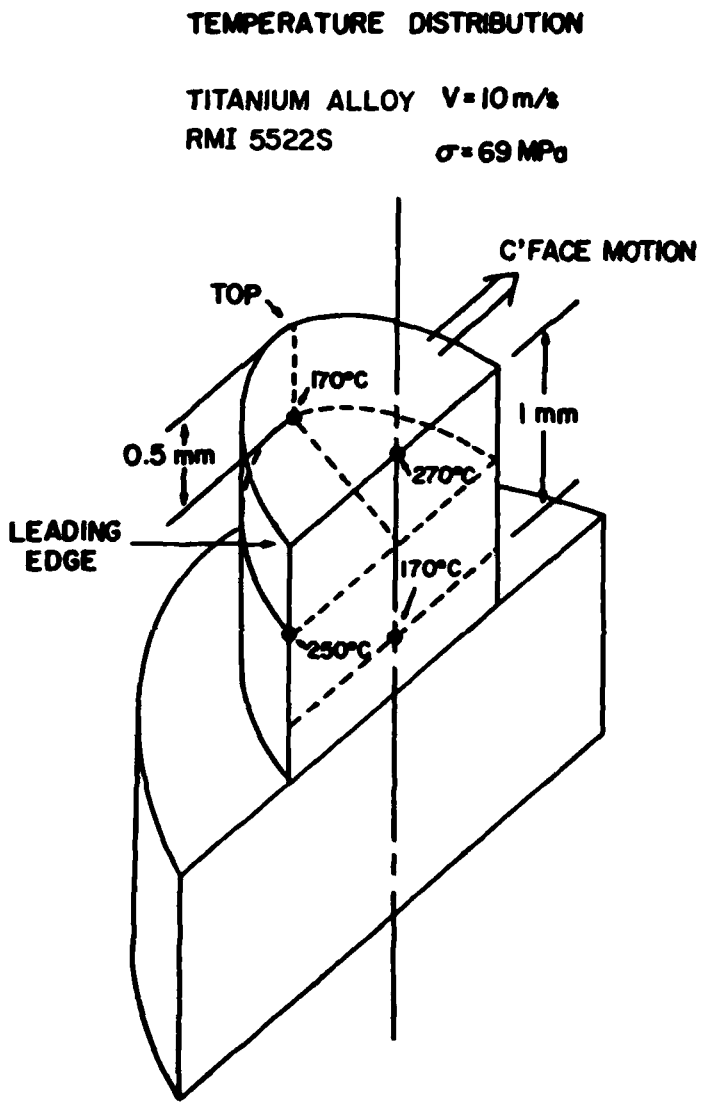

Fig. 10

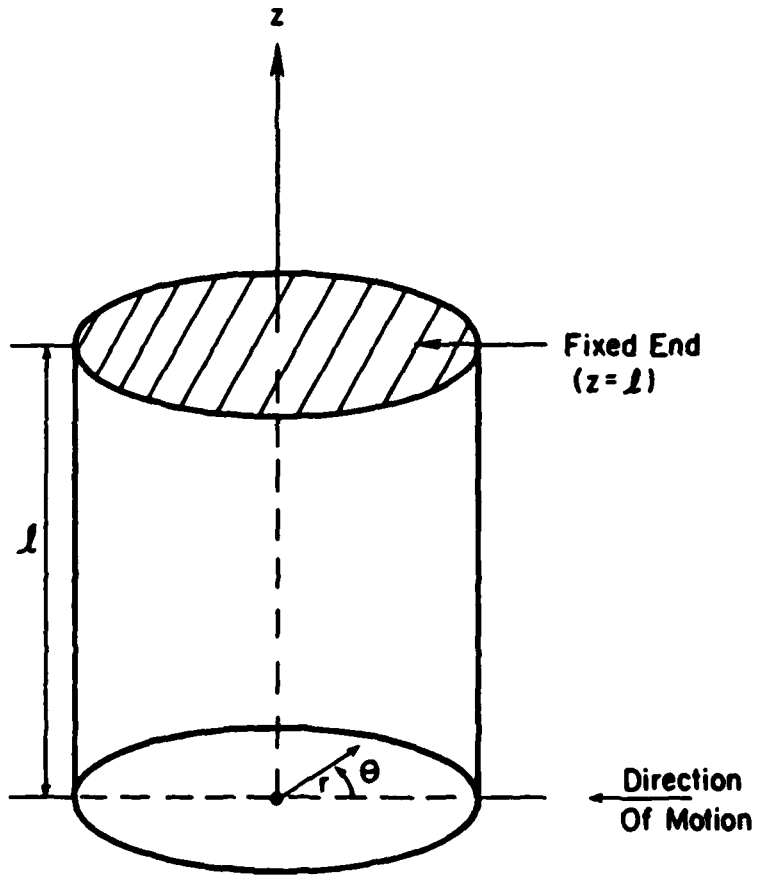

Fig. 11

Geometry Of The Cylinder

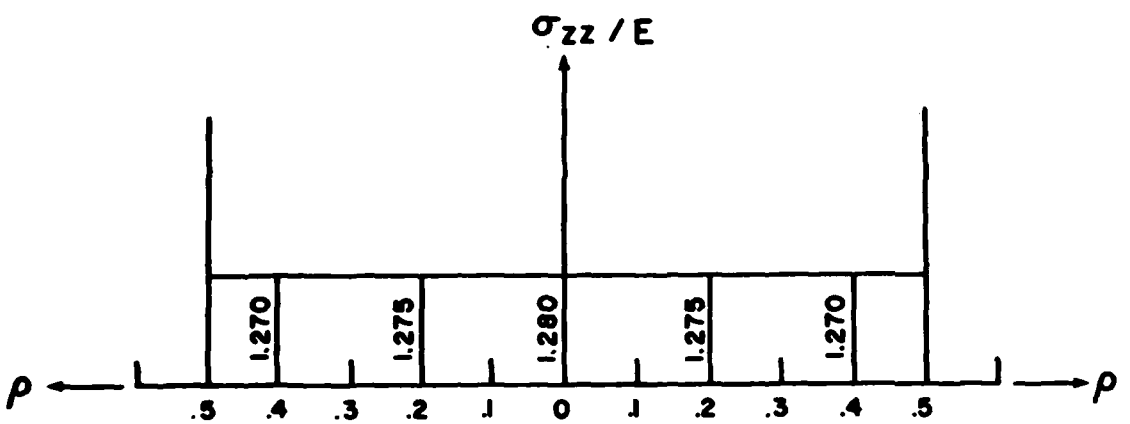

Fig. 12

Normal Stresses Along The Diameter Of The Interface;
k = 0

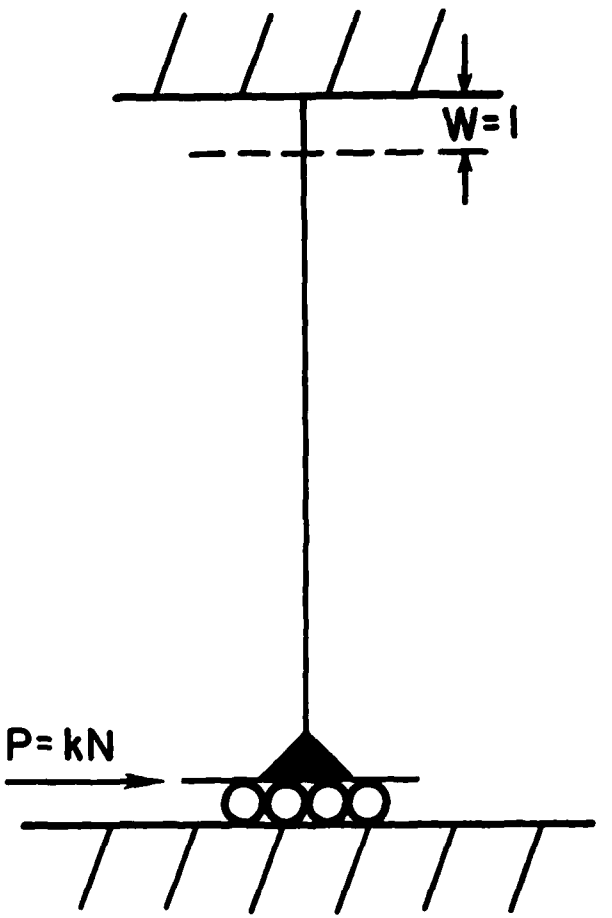

Fig. 13

A Simple Model

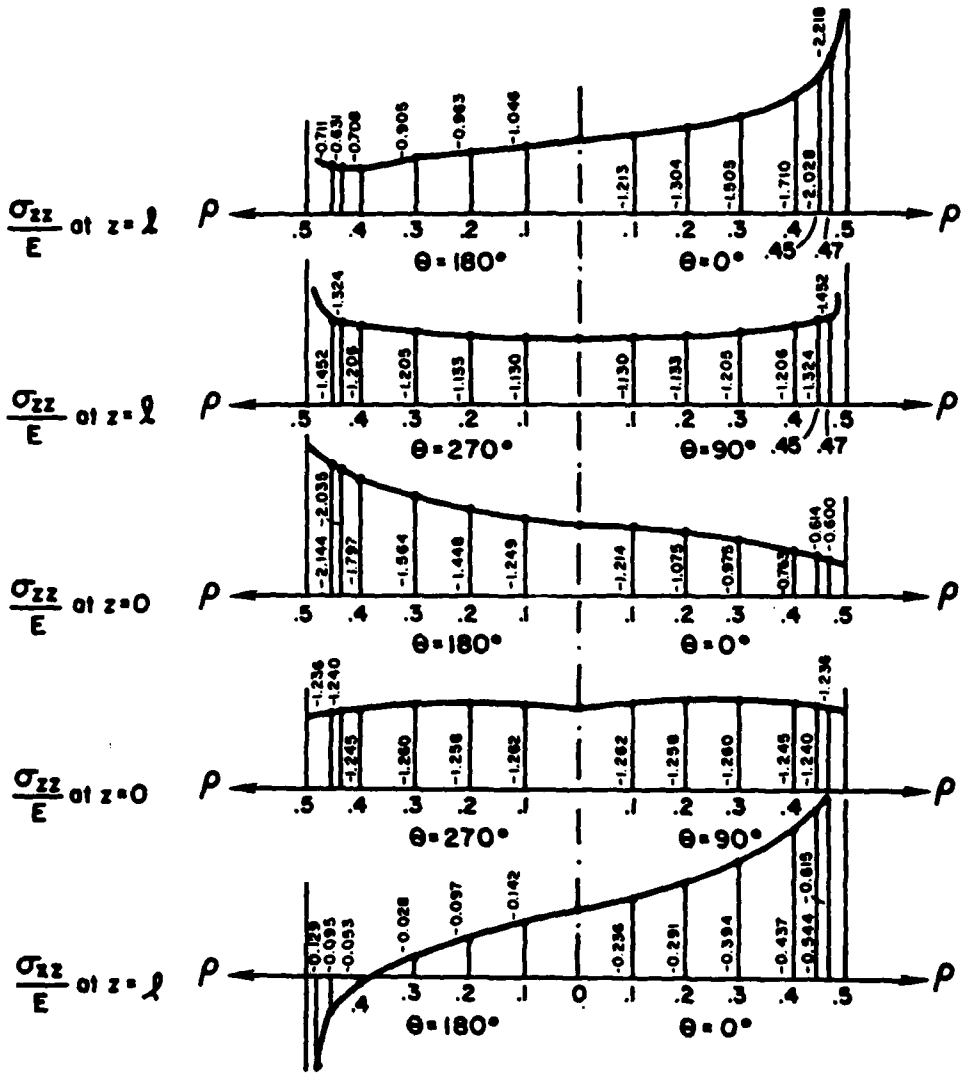

Fig. 14

Stresses At The Flat Ends Of The Cylinder For k=0.15

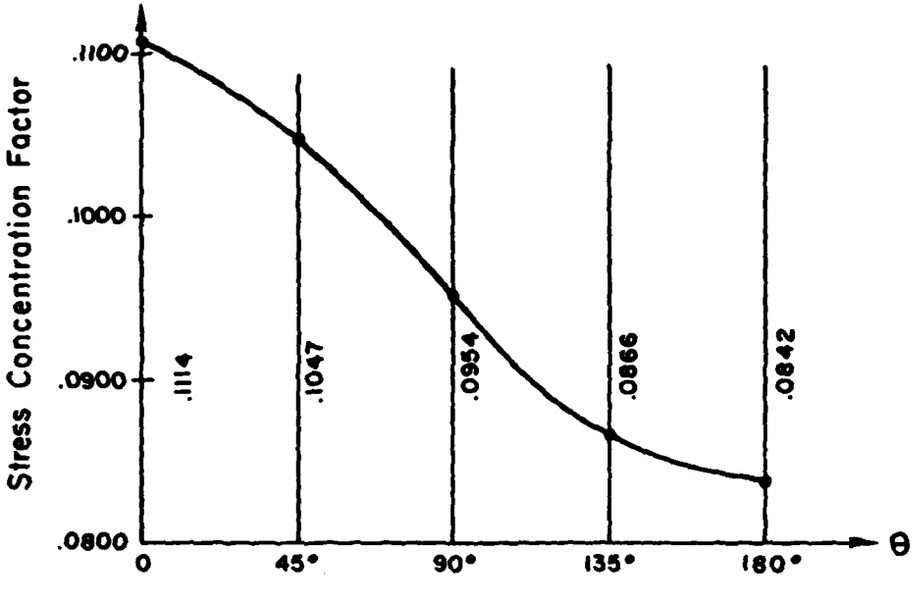

Fig. 15

Variation Of The Stress Concentration Factor With The Angle θ (k = 0.15)

INSTITUTE OF MATERIALS SCIENCE

The Institute of Materials Science (IMS) was established at The University of Connecticut in 1966 in order to promote academic research programs in materials science. To provide requisite research laboratories and equipment, the State of Connecticut appropriated $5,000,000, which was augmented by over $2,000,000 in federal grants. To operate the Institute, the State Legislature appropriates over $500,000 annually for faculty and staff salaries, supplies and commodities, and supporting facilities such as an electronics shop, instrument shop, a reading room, etc. This core funding has enabled IMS to attract over $2,500,000 annually in direct grants from federal agencies and industrial sponsors.

IMS fosters interdisciplinary graduate programs in Alloy Science, Biomaterials, Corrosion Science, Crystal Science, Metallurgy, and Polymer Science. These programs are directed toward training graduate students while advancing the frontiers of knowledge and meeting current and long-range needs of our state and our nation.

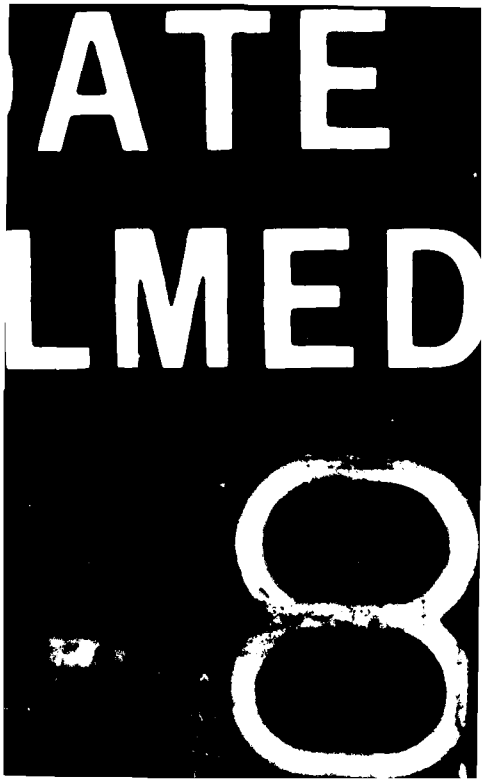
ATE
LMED
8